IAC-13,B5,2.8x19167

# INTEGRATED END-TO-END NEO THREAT MITIGATION SOFTWARE SUITE

**Juan L. Cano**
Elecnor Deimos, Tres Cantos, Spain, juan-luis.cano@deimos-space.com

**Gabriele Bellei**
Elecnor Deimos at ESOC, Darmstadt, Germany, gabriele.bellei@esa.int

**Javier Martín**
Elecnor Deimos, Tres Cantos, Spain, javier.martin@deimos-space.com

Protecting Earth from the threat implied by the Near Earth Objects (NEO) is gaining momentum in recent years. In the last decade a number of mitigation methods have been pushed forward as a possible remedy to that threat, including nuclear blasts, kinetic impactor, gravity tractors and others. Tools are required to evaluate the NEO deflection performances of each of the different methods, coupled with the orbital mechanics associated to the need to transfer to the target orbit and maybe rendezvous with it. The present suite of tools do provide an integral answer to the need of determining if an asteroid is to collide with Earth (NIRAT tool), compute the required object deflection (NEODET tool) and assess the design features of the possible mitigation space missions (RIMISET tool). The tools are presented, their design analyzed as well as the methods and architecture implemented. Results are provided for two asteroids 2011 AG5 (using the orbit determination solution where this asteroid still was a risk object) and 2007 VK184 and the obtained data discussed in comparison to other results.

## I. INTRODUCTION

Currently, there are a number of institutions worldwide that contribute to the discovery, tracking, identification, cataloguing and risk characterization of asteroids in general, and NEOs in particular. However, there is no currently an integrated set of tools that cover in a complete manner the assessment of the impact risk mitigation actions that can be taken to prevent the impact of a NEO on Earth and to allow helping the dimensioning of space missions to address such problem.

Within the EC funded NEOShield project[*] started in 2012 the following set of utilities has been developed. Those allow covering the abovementioned activities:

- NEO Impact Risk Assessment Tool (NIRAT).
- NEO Deflection Evaluation Tool (NEODET).
- Risk Mitigation Strategies Evaluation Tool (RIMISET).

NIRAT, the first tool, allows evaluating the projection of the b-plane dispersion at the dates of possible impact for likely impactors and also the presence of keyholes that would enable future collision opportunities. This tool allows characterizing the impact probability for the different opportunities and, together with the knowledge of the asteroid features, the evaluation of the risk in terms of the Palermo Scale and the Torino Scale. This tool resembles current performances achieved by NEODyS[1] and Sentry[2], but does not intend to represent the same level of accuracy in the obtained results. The services provided by this tool are required by the next other tools.

The second tool, NEODET, allows assessing the required optimal change in asteroid velocity (modulus and direction) at any given instant prior to the possible impact epoch that would allow shifting the dispersion ellipse out of the contact with the Earth. This by means of impulsive mitigation options (one or several impacts) and by the accumulated effect that slow-push techniques (e.g. gravity tractor) could impose on the asteroid orbit to achieve optimal deflection.

Finally, the RIMISET tool allows evaluating how each of the possible impulsive and slow-push mitigation techniques would meet the required changes in asteroid state to obtain the searched for deflection and the requirements that this could impose on the design of the mitigation mission. Each technological solution would be simulated to allow ascertaining the efficiency in achieving the goal deflection by any of the proposed means (impact, explosive, gravity tractor and possible combinations of those). Ultimately, it serves to dimension the required mitigation space systems and solutions.

The research leading to these results has received funding from the European Community's Seventh Framework Programme (FP7/2007-2013) under grant agreement n° 282703.

[*] See www.NEOShield.net

## II. THE NEO RISK ASSESSMENT TOOL - NIRAT

The NEO Risk Assessment Tool (NIRAT) is a piece of software aimed at the identification of potential future collision threats from Near Earth Objects.

When a new asteroid is discovered and its orbit is estimated, relevant uncertainties on the accuracy of the orbit determination (OD) solution may be present[3,4]. This means that the actual evolution of the NEO orbit could deviate significantly from the reference solution. If intermediate planetary encounters are present, they can contribute in amplifying the size of the uncertainty region at the epoch of the threat, possibly increasing the risk on Earth. It is thus fundamental to evaluate as many as possible different trajectories compatible with the uncertainty domain, in order to identify the ones which may collide with the Earth and to provide a statistical evaluation of the risk.

The state of the art tools for asteroid OD and collision risk monitoring are CLOMON2[5,6], managed by university of Pisa together with other institutions and Sentry[7], operated by JPL. NIRAT is not meant to achieve the same level of accuracy and completeness of those systems, but aims at evaluating, by the means of simple algorithms and with minimum intervention by the user, the risk of possible future impacts, providing a quick assessment tool to support system-level studies for hazard mitigation missions.

### II.I. Tool Description

NIRAT software is an integrated tool combining some well known astrodynamical techniques in a simple and easy to use environment. In the following paragraphs the main aspects of the adopted techniques are briefly summarized. Among those techniques stand the Monte Carlo sampling and the Line of Variations sampling.

#### II.I.i. Orbit Propagator

The core of NIRAT tool consists in a Cowell orbit propagator, based on a variable step Runge-Kutta-Fehlberg 7(8) integration scheme[8]. The center of integration is the Sun, but whenever the sphere of influence of a planet is entered, the central body is automatically changed to preserve numerical accuracy. Gravity from the planets can be treated with point-mass or spherical harmonics models, and their positions and velocities are obtained by ephemeris reading and interpolation (no integration of planetary motion). The gravitational effect of the major asteroids is also considered in the propagation. A basic modeling of relativistic effects is included, considering the Sun monopole term only[9]. Solar radiation pressure is treated with a simplified radial model. The implementation of the Yarkovsky effect is foreseen as a major update to the propagator in the future. To enhance tool flexibility, instantaneous changes of velocity or continuous accelerations on the asteroid can be applied to simulate fast and slow push mitigation techniques.

#### II.I.ii. Monte Carlo Sampling

The Monte Carlo (MC) engine permits to propagate a multitude of possible asteroid orbits, called Virtual Asteroids (VAs), all compatible with a certain OD solution. An OD solution consists in a set of orbital elements given at a specified epoch, and an associated uncertainty region, which in general can have a curved shape, but for many practical applications can be well approximated by a 6-dimensional ellipsoid defined through a covariance matrix. The MC sampling method implements a random perturbation of all (or some) of the orbital elements, based on a multivariate normal distribution obtaining the covariance matrix from the mentioned OD solution. Perturbations are derived by using a normal random generator, based on a Mersenne twister algorithm[10] and a Box-Muller transform[11], which is considered to have a sufficiently accurate statistical behavior. Custom scaling can be applied to the covariance matrix prior to the calculation of eigenvalues/eigenvectors, to improve numerical conditioning. Different parameterization can be used for the definition of initial state and covariance, such as Keplerian elements, position/velocity state vector, cometary and equinoctial elements, to allow compatibility with different formats of OD solutions.

During propagation, all planetary close encounters are tracked, for b-plane analysis, keyhole identification and risk probability computation for those trajectories ending with a collision, named Virtual Impactors (VIs).

#### II.I.iii. Line of Variations Sampling

Although very simple and effective, Monte Carlo sampling is also very intensive in terms of computational resources if statistical accuracy is required. With impact probabilities lower than $10^{-4}$ and tens of years propagations the problem results too heavy to be practically affordable on standard processors.

The concept of Line of Variations[5,12] is based on the idea that the uncertainty region associated with an OD solution has typically an elongated shape, especially when the asteroid observations are sufficiently separated in time. When propagated over very long time spans, different solutions belonging to the uncertainty domain spread in true anomaly, and the uncertainty region becomes a very elongated, curved and thin tube which may even include the entire orbit. A sampling along a one-dimensional subspace of the initial uncertainty region, following the weakest direction of the OD solution, may be sufficient to capture the essence of the multiplicity of the solutions. This one-dimensional space is called Line of Variations (LOV), it is generally curved and it can have different mathematical formulations[5], but in many practical cases it is well

approximated by the major axis of the covariance ellipsoid of the reference OD solution. This last simplified version of LOV is implemented in NIRAT, and can be efficiently sampled with a limited number of points for the search of virtual impactors.

II.I.iv. B-plane Analysis

A target plane represents a meaningful approach to study the geometry of a close encounter between a minor body and a planet[3,4]. In general it is defined as a planet-centered plane perpendicular to the relative body-planet velocity at some interest point. In particular, the b-plane is defined as the plane perpendicular to the incoming asymptotic velocity of the asteroid trajectory, which is in the vast majority of cases hyperbolic. Different definitions of the in-plane coordinate axes are possible[4]; for NIRAT, the b-plane coordinate system is defined by a ($\xi$, $\eta$, $\zeta$) tern, where $\eta$ is the direction of the asymptotic incoming velocity, $-\zeta$ along the projection of heliocentric velocity of the planet and the remaining axis, $\xi$, completes the right-handed tern. With this useful representation, a family of different solutions, belonging to the uncertainty region, can be represented on the b-plane, where the $\xi$ coordinate is a measure of the Minimum Orbital Intersection Distance (MOID), nearly constant for a given encounter, and the $\zeta$ axis gives a measure of the timing of the encounter (if positive, the asteroid is late, and vice-versa). The existence of virtual asteroids with $\xi$ less than Earth radius, corrected by the gravitational focusing effect due to hyperbolic motion, is by itself an indicator of a potential risk that needs to be evaluated in detail. Whenever the impact vector ($\xi$, $\zeta$) is contained within the Earth disc, a virtual impactor is found.

In the case of resonant close approaches, b-plane analysis permits also to detect possible keyholes for future impacts. Keyholes can be thought as the projection of the Earth shape at a future encounter back on the b-plane of the current one: if the asteroid passes through one of them, an impact will occur at some future date. It is thus fundamental to characterize their position and size, which is valuable information for the study of mitigation missions in case a high-probability collision is found.

II.II. Results

To validate the methods implemented in NIRAT, two different study cases were considered, involving the two asteroids that, at the time of tool development (end of 2012), reported a non-null value of the impact risk on the Torino scale[13]: asteroid 2011 AG5, having a collision probability of about 1/500 in 2040, and asteroid 2007 VK184, with an impact probability of about 1/1800 in 2048.

The first belongs to the Apollo class in terms of orbital properties, having a semi-major axis of about 1.43 AU and an eccentricity of about 0.39. The orbital elements were computed based on 213 astrometric observations, spanning a period of 317 days[2]. A close approach with the Earth is foreseen for 3rd February 2023, at an approximate distance of 1.85 Mkm. Although such a distance is not very close to Earth, it is sufficient to generate a noticeable uncertainty in the orbital elements following the encounter. The possibility of an Earth impact on 5th Feb. 2040 was foreseen by the main hazard monitoring systems with a relatively high probability (1/500), making the asteroid hit the value 1 on the Torino Scale and bringing it to the media attention. The advent of new observations at the end of 2012 ruled out any possible risk in 2040, nevertheless the asteroid represented a very interesting study case.

Asteroid 2007 VK184 also belongs to the Apollo class in terms of orbital properties, with a semi-major axis of about 1.73 AU and an eccentricity of about 0.57. The orbital elements are based on 101 astrometric observations[2], spanning a period of 60 days only. A close approach with Earth is foreseen on 30th May 2048, at an approximate reference distance of 4.8 Mkm. Although the reference trajectory passes quite far from Earth, the uncertainty on orbital parameters allows the existence of virtual impactors, identified by both Sentry and CLOMON2 for 3rd June 2048 with a probability of about 1/1800.

For both study cases, the two different sampling methods available in NIRAT were applied. MC simulations were performed with 10,000 virtual asteroids, with a sampling over a 6-dimensional multivariate normal distribution in orbital elements. LOV sampling were performed with 1,001 equally spaced virtual asteroids, between $-3\sigma$ and $3\sigma$ values on the largest axis of the uncertainty covariance ellipsoid. Initial epoch, orbital elements and full covariance matrix were obtained from JPL NEO page[2] and from NEODyS page[1], as available in September 2012. Initial conditions were propagated up to a few days after the date of the nominal encounter, including all the perturbing effects defined in the so called Standard Dynamic Model[14]: gravity from all planets, the Moon, Ceres, Pallas and Vesta (as point masses) and the relativistic gravitational effects.

II.II.i. Asteroid 2011 AG5 Study Case

The case of asteroid 2011 AG5 is the most complex to analyze, since it represents the typical situation of resonant encounters, the first in 2023 being a possible keyhole for a future impact in 2040. The OD solution leading to a possible collision in 2040 was used.

In Fig. 1 a magnified portion of the 2023 b-plane is represented in the proximity of the keyhole, showing the virtual impactors marked in red. The keyhole extends for about 360 km in the vertical direction, while the

uncertainty region is approximately 40-50 km wide. In Fig. 2, a visualization of the 2040 encounter on the b-plane is represented, comparing the results from MC and LOV sampling, in the vicinity of the crossing between the uncertainty region and the Earth shape projected on the plane. It is possible to see the 16 virtual impactors found by MC sampling (top plot) and the very accurate description of the encounter geometry with LOV sampling (bottom plot). Despite the reduced number of samples, LOV analysis permits to easily identify the existence of impactors for the case under exam. While MC sampling takes about 25 h (on a standard office PC, 2.5 GHz processor, 2 GB RAM), LOV sampling needs only 2.5h.

In Table 1 the results obtained by NIRAT with MC and LOV sampling are summarized and compared with Sentry and CLOMON2 results[7,6], although the analysis was initialized with Sentry OD solution in this case. The 2040 close approach for the nominal trajectory is identified at the right epoch, with an error in the minimum distance of only 75 km after a 28-year time span. The impact probability, although not identical, is close to the one calculated by JPL, despite the necessarily limited number of samples, not sufficient to ensure an accurate probability computation. The position of the impact solutions along the LOV have a sigma value of -0.282, which compares very well with the Sentry solution, found at 0.281 sigma.

II.II.ii. Asteroid 2007 VK184 Study Case

The second validation case, related to asteroid 2007 VK184, is simpler to study as no intermediate close encounter occurs before the epoch of the foreseen hazard. The problem can be studied then directly in the b-plane of the 2048 encounter.

In Fig. 3 a visualization of the encounter on the b-plane is shown for MC and LOV sampling. A number of 6 virtual asteroids fall within the projection of the Earth sphere, indicating a probability of about 1/1667. Although LOV sampling does not identify directly any VI, the existence of impact solutions can be easily seen by simply inspecting the bottom plot. In the absence of an appropriate root finder, a virtual impactor solution can be quickly recovered manually, knowing the points along the LOV that delimit the horizontal axis crossing. It can be observed that in this case the projection of the uncertainty region on the b-plane is thicker, with a width of about 200 km, due to a poorer OD solution and a longer propagation time.

In Table 1 the solutions obtained by NIRAT are again compared with CLOMON2 and Sentry results[7,6]. In this case the agreement with CLOMON2 is better, as this was chosen as the source for orbital elements and covariance. The close approach in 2048 is correctly identified, and the impact probability is compatible with the one obtained by CLOMON2, with the usual caveats on the validity of statistics with only 6 VIs. The sigma position of the impact solutions along the LOV shows excellent agreement, while the difference in the distance of closest approach, about 0.75 Earth radii for NIRAT and Sentry and 0.92 for CLOMON2, is due to the Earth scaling for the focusing effect in NIRAT and Sentry.

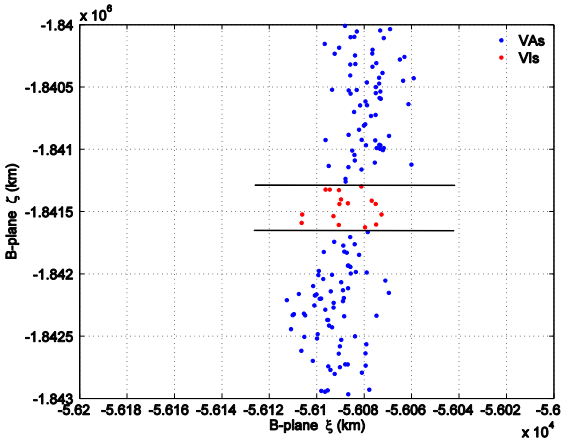


Fig. 1: Representation of 2023 keyhole for asteroid 2011 AG5.

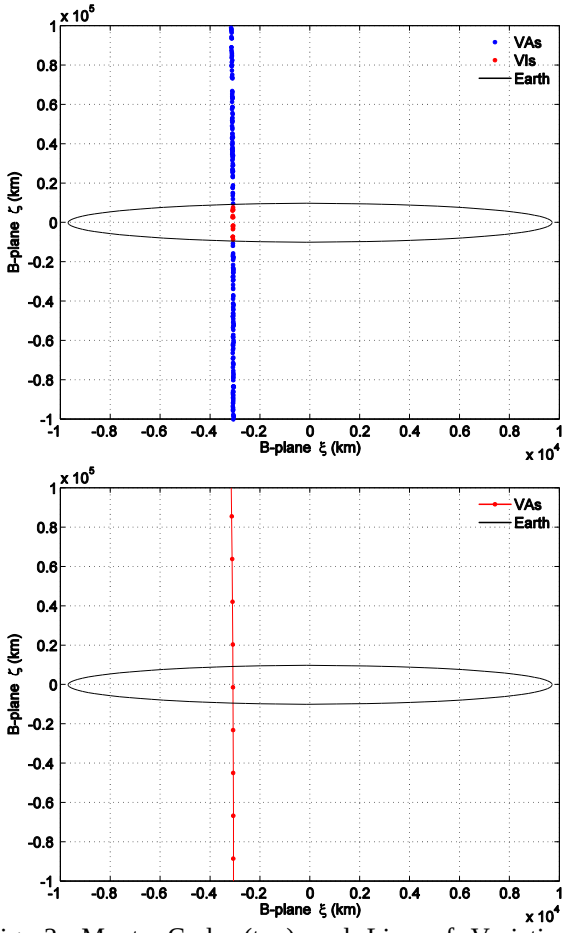


Fig. 2: Monte Carlo (top) and Line of Variations (bottom) comparison on 2040 b-plane for asteroid 2011 AG5.

| Asteroid 2011 AG5 | NIRAT | Sentry | CLOMON2 |
|---|---|---|---|
| Reference epoch for 2040 close encounter (MJD2000) | 14644.402 | 14644.401 | 14644.675 |
| Reference distance of 2040 close approach (km) | 1.033067e6 | 1.033142e6 | 6.63885e5 |
| Epoch of impact solution (MJD2000) | 14645.161 | 14645.16 | 14645.163 |
| MC number of virtual impactors (over 10000 shots) | 16 | - | - |
| Impact probability | 1/625 | 1/500 | 1/552 |
| MC distance of closest approach on b-plane (Earth radii) | 0.32 | 0.31 | 0.48 |
| LOV sigma position of closest approach | -0.282 | 0.281 | -0.163 |
| Asteroid 2007 VK184 | NIRAT | CLOMON2 | Sentry |
| Reference epoch for 2048 close encounter (MJD2000) | 17683.811 | 17683.811 | 17683.795 |
| Reference distance of 2048 close approach (km) | 4.757776e6 | 4.757720e6 | 4.792016e6 |
| Epoch of impact solution (MJD2000) | 17686.089 | 17686.089 | 17686.09 |
| MC number of virtual impactors (over 10000 shots) | 6 | - | - |
| Impact probability | 1/1667 | 1/1801 | 1/1818 |
| MC distance of closest approach on b-plane (Earth radii) | 0.75 | 0.92 | 0.75 |
| LOV sigma position of closest approach | 1.293 | 1.296 | 1.322 |

Table 1: Comparison between NIRAT, Sentry and CLOMON2 results for asteroid close encounters.

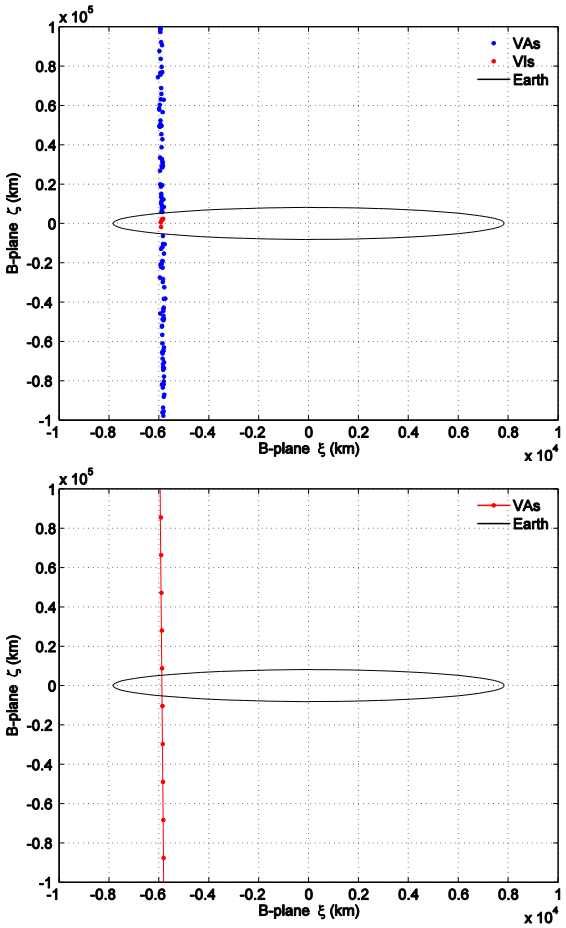


Fig. 3: Monte Carlo (top) and Line of Variations (bottom) comparison on 2048 b-plane for asteroid 2007 VK 184.

II.III. Discussion

The presented results show that, despite the necessary simplifications needed to develop a new tool in a few months and with limited resources, it was possible to achieve accuracy in the numerical modeling of asteroid dynamics close to the current state of the art. If the geometry of the uncertainty region is not made too complex by multiple deep planetary encounters, it is possible to assess with limited effort the risk of impact for time spans of the order of decades. One of the main difficulties, which also remains an open point for NIRAT, is the inclusion of an accurate modeling of solar radiation pressure and asteroid radiative effects in general[14,15]. In fact, these effects mainly depend on the physical properties of the asteroid, especially mass, shape, surface, reflection and absorption coefficients, together with its rotational state. This information in most cases is not available with standard optical and radio observations of faint objects, and would require dedicated characterization missions to be known with sufficient detail. In particular, the Yarkovsky effect, related to the emission of thermal radiation in the direction of asteroid motion, can be a main player because it directly affects the orbital period and thus the timing of an encounter, especially for smaller objects and in presence of keyholes of reduced size. The foreseen inclusion of these effects in the uncertain parameters set for statistical computation will surely improve the robustness of the risk estimation.

## III. THE NEO DEFLECTION TOOL - NEODET

The second tool in the set, NEODET, focuses on the exploration of orbital dynamics constraints in a possible deflection mission of an asteroid that has previously been identified as a threat by NIRAT. The tool supports two different types of deflection attempts:

1. Impulsive problems: a nearly instantaneous change in the asteroid velocity without a change in position. This case models events such as the crash of a kinetic impactor or a nuclear blast.

2. Continuous problems: a force applied over a period of time long enough to span a significant part of the NEO orbital period. Examples are the gravity tractor and the ion-beam shepherd methods.

In each case, the program allows the evaluation of either the direct or the inverse problem. In the former, the input consists of a description of the introduced perturbation (e.g. the imparted $\Delta\mathbf{v}$ for an impulsive problem) while the output is the associated b-plane deflection. For inverse problems, however, the input is the desired b-plane displacement and the output is an optimal perturbation that produces the requested deflection. Furthermore, an additional inverse case is provided for impulsive deflections, see III.I.ii.

III.I. Description

Most of the logic in the tool revolves around the propagation of selectively perturbed virtual impactors, often within the context of an optimization of some function of the perturbation parameters. The particular algorithm is different for each problem, as described in the following sections.

III.I.i. NEO Modeling and Orbital Propagation

To the effects of this tool, all NEOs are modeled as dimensionless points, with inertial mass but no gravity of their own. The main propagation model is the same used in NIRAT.

An alternative propagation model is provided for continuous thrust problems, based on the analytical solution described by Bombardelli and Baù[16]. The NEODET implementation employs the simple expression for the spatial lag $\Delta\zeta$, which provides a good enough level of approximation; but includes expansions up to order 8 of the MOID $\Delta\xi$. The implementation of some functions required the computation of complete elliptical integrals of the first and second kinds, based on the method described by Adlaj[17].

III.I.ii. The Impulsive Problem

The perturbation is modeled as an instantaneous velocity change $\Delta\mathbf{v}$ over the state vector $\mathbf{x}$, applied to the NEO at a certain point in time $t_b$. All problem subtypes are based on the *b-plane displacement function*, $\Delta\mathbf{b}(\Delta\mathbf{v}, t_b)$, which evaluates the change in the b-plane representation of the close approach (CA) when the perturbation is applied:

$$t_0, \mathbf{x}_0 \rightarrow \begin{cases} t_{CA0}, \mathbf{x}_{CA0} \Rightarrow \mathbf{b}_0 \\ t_b, \mathbf{x}_b \rightarrow t_b, \tilde{\mathbf{x}}_b \rightarrow t_{CA}, \mathbf{x}_{CA} \Rightarrow \mathbf{b} \end{cases} \qquad [1]$$

$$\Delta\mathbf{b}(\Delta\mathbf{v}, t_b) = \mathbf{b}(\Delta\mathbf{v}, t_b) - \mathbf{b_0}$$

The impulsive direct problem is a simple application of the above definition, as the input consists of the impulse to apply and the time of the deflection. In the hybrid case, the input is an admissible impulse magnitude $\Delta\mathbf{v}$ applied at a time $t_b$, and the result is the orientation that will produce the largest b-plane displacement. In other words, an optimization problem on the impulse $\mathbf{u}$, where the magnitude of $\Delta\mathbf{b}$ from [1] is the function to maximize:

$$\max_{\mathbf{u}} \left\| \Delta\mathbf{b}(\mathbf{u}; t_b) \right\| \quad / \quad \left\| \mathbf{u} \right\| = \Delta v_{req} \qquad [2]$$

A similar reasoning applies to the inverse case, where the input is a desired b-plane displacement $\Delta b$ produced by an impulse at a time $t_b$, and the result is the smallest impulse $\mathbf{u}$ fulfilling the constraint:

$$\min_{\mathbf{u}} \left\| \mathbf{u} \right\| \quad / \quad \left\| \Delta\mathbf{b}(\mathbf{u}; t_b) \right\| = \Delta b_{req} \qquad [3]$$

In both cases, the optimization procedure employs a non-linear recursive quadratic programming method.

Finally, it can be mentioned that some special cases can occur that need a special treatment:

1. The disturbed NEO trajectory might not have a close approach to the body at a date near the original: as this is the effect of an excessive deflection, $\Delta\mathbf{b}$ is defined to evaluate to infinity.

2. Other eventualities, such as an impact on a different body; or the same but in a date too far off that of the unperturbed case. The value of the displacement function is then undefined, which is represented with the special value of "not a number" (NaN).

III.I.iii. The Continuous Problem

The perturbation is modeled in this case as a force $\mathbf{F}$ applied between two instants of time $t_b$ and $t_f$. The treatment and form of the force depends on the selected solver: the analytical approximation described in III.I.i limits the force to a constant tangential thrust, but the numerical integrator can use a more generic model:

$$\mathbf{F}(\mathbf{x}, t) = F(r_{Sun}(\mathbf{x}))\, \mathbf{A}_{i0}(t) \cdot \mathbf{u}_{\mathbf{F}} \qquad [4]$$

Where $\mathbf{A}_{i0}$ is the rotation matrix from one of the defined reference frames (see below) and $\mathbf{u_F}$ is a constant unit vector. There are essentially three generic degrees of freedom:

1. The model of the thrust magnitude, either constant or dependent on a power of the distance to the Sun.

2. The orientation of the force, given as constant right ascension and declination values.

3. The base frame, which may be the ICRF, the orbital perifocal frame or the trajectory intrinsic frame.

In the continuous case, the b-plane displacement function for a particular force model is defined as $\Delta\mathbf{b}$ ($t_f$, $t_b$). The analytic model provides explicit formulas for ($\Delta\xi$, $\Delta\zeta$), while in the numerical propagator the force described above is incorporated as another perturbation

to the integration. The function is evaluated in a similar way as in [1], and with the same special cases mentioned there. Also, like in the impulsive case, the continuous direct problem is solved by the direct application of the b-plane displacement function.

The definition of the "inverse case", on the other hand, is not unique because several parameters could be chosen as outputs. The formulation in NEODET returns the minimum time $t_f$ (for a fixed $t_b$) that is needed to successfully deflect the NEO by the requested amount on the b-plane. The implementation *assumes* that $|\Delta\mathbf{b}|$ is roughly monotonic in $t_f$, removing the need for the optimization. Instead, the tool solves:

$$\left\|\Delta\mathbf{b}(t_f;t_b)\right\| = \Delta b_{req} \qquad [5]$$

For $t_f$ values between $t_b$ and the forecast impact date $t_{CA0}$. The implementation employs a bisection-like algorithm, which allows the tool to determine *a priori* (under the mentioned assumption of monotonicity) whether the requested deflection is at all possible and save time if it is not.

The mentioned assumption of monotonicity in $\Delta\mathbf{b}(t_f, t_b)$ amounts to stating that the secular drift terms are the main drivers of the solution and that continued pushes keep affecting the b-plane in roughly the same direction. If the NEO swings by a massive body in the thrust arc, the latter condition may not hold, since the modified orbit may cause pre- and post-flyby pushes to affect the b-plane in significantly different directions.

As an example, fig. 4 shows a series of deflection missions for 2011 AG5, which has a close approach to Earth in early 2023. Keeping the thrust on after or even shortly before the flyby causes a *reduction* in the achieved performance in the propagation (the analytic solution is completely erroneous, as expected by the method limitations).

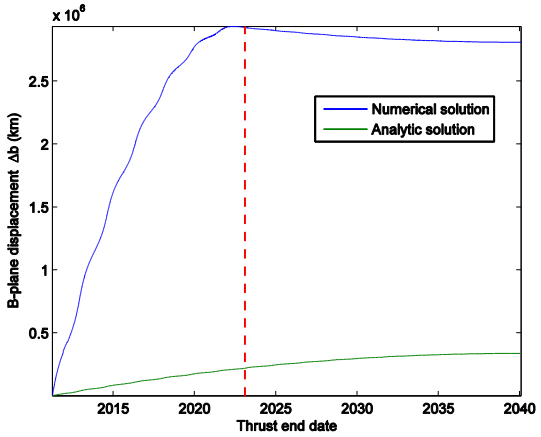


Fig. 4: Continuous deflection missions for 2011 AG5 started before the 2023 flyby.

III.II. Results

The asteroids for the NEODET test cases are the same used for NIRAT. The virtual impactor for each NEO is obtained from the nominal conditions by using NIRAT to sample the line of variations and choosing the virtual asteroid with $\zeta = 0$.

III.II.i. Impulsive Deflections

In this section, the same two cases are analyzed with the impulsive inverse method. A desired deflection of one Earth radius in the b-plane is fixed and the tool is asked to investigate the required impulse $\Delta\mathbf{v}(t_b)$ for each date in a given time interval. Since the numerical optimization may fail to converge at some time points, each case also includes the plot of the obtained b-plane deflection as verification. This plot should be constant for converged cases but will deviate from the requested value for cases that do not converge.

Fig. 5 and fig. 7 represent the obtained deflection requirement ($\Delta\mathbf{v}$) for 2007 VK184 and 2011 AG5, respectively, as a function of the date of the deflection attempt. Fig. 6 and fig. 8 contain the magnitude of the obtained deflection for both asteroids; as mentioned, in the impulsive inverse case these plots serve as a check on the values of the corresponding $\Delta\mathbf{v}$ graphs. The results obtained for 2011 AG5 match very well the ones obtained by Bellei and Cano[18] with a slightly different approach.

The irregular evolution of the out-of-plane component in plots Fig. 5 and fig. 7 is due to the current level of accuracy requested to the optimization process, being of a similar order as this component size.

III.II.ii. Continuous Deflections

Fig. 9 and fig. 10 show the result of a continuous deflection of 2011 AG5 and 2007 VK184, respectively.

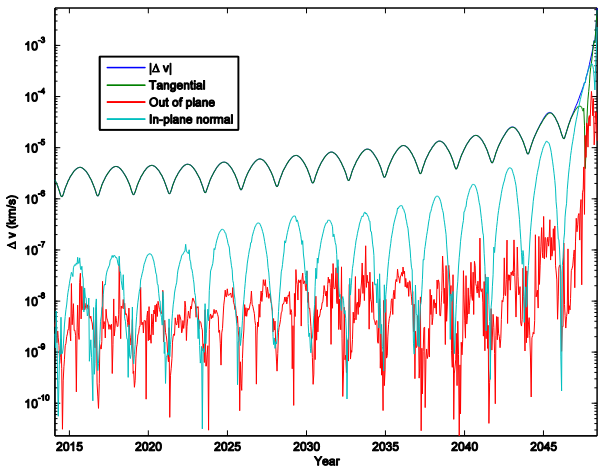


Fig. 5: $\Delta\mathbf{v}$ required to deflect 2007 VK184 by one Earth radius in the 2048 close approach.

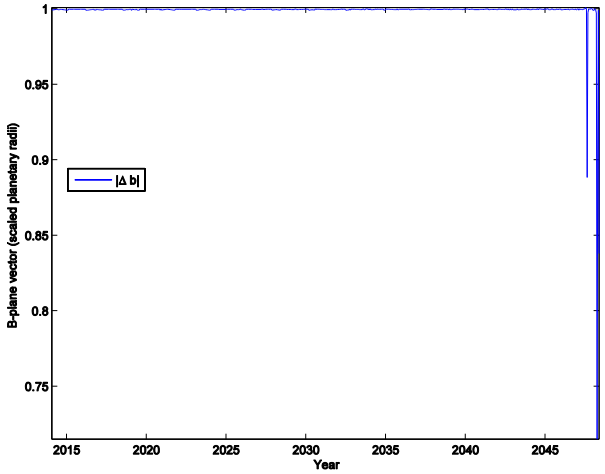


Fig. 6: B-plane displacements actually obtained in the 2007 VK184 deflection attempt.

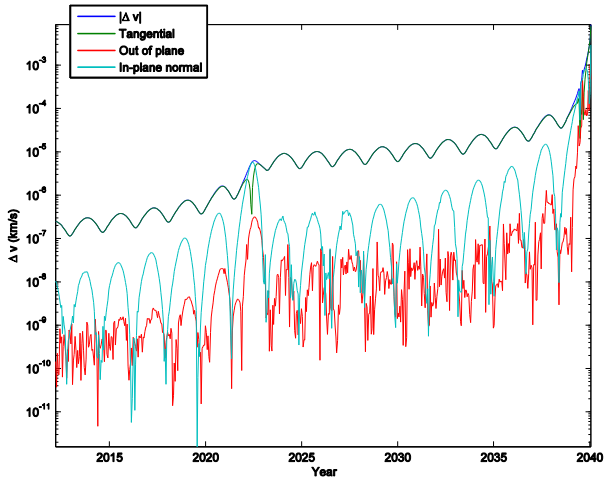


Fig. 7: Δ**v** required to deflect 2011 AG5 by one Earth radius in the 2040 close approach.

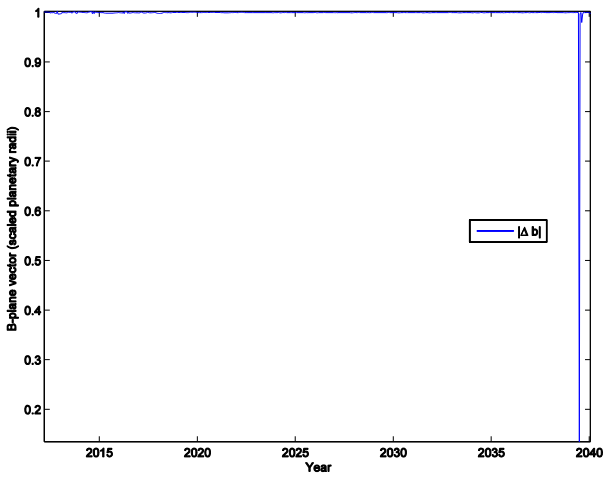


Fig. 8: B-plane displacements actually obtained in the 2011 AG5 deflection attempt.

The NEO masses, needed for the computation of the asteroid acceleration, have been approximately derived from known properties of the asteroid. The values used in the simulations were $3.9 \cdot 10^9$ kg for 2011 AG5 and $3.3 \cdot 10^9$ kg for 2007 VK184.

The data has been generated using the continuous direct problem type, with four cases run for each NEO accounting for the two different solvers and two types of thrust arcs.

All cases have been computed using a constant tangential thrust of magnitude 1 N acting on the asteroid, with $t_b$ starting ten years before the respective forecast impact dates. The two cases represented as dashed lines have used a thrust arc limited to at most two years, letting the NEO coast to the close approach after that, if date of the impact was further away than the mentioned two years. The other two, pictured as solid lines, have kept the force acting until the date of the impact.

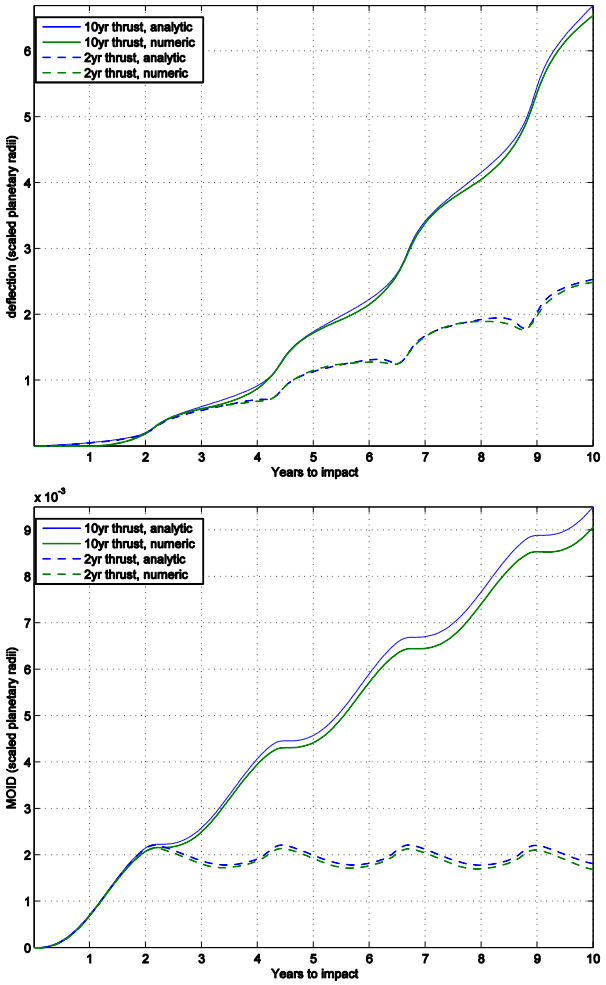


Fig. 9: B-plane deflection of 2007 VK184 with four different continuous deflection set-ups.

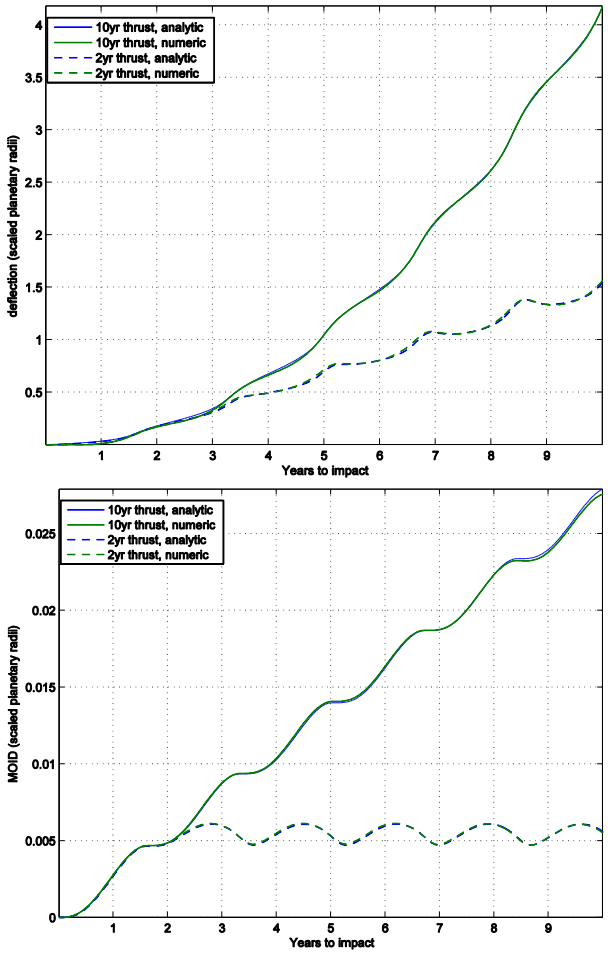


Fig. 10: B-plane deflection of 2011 AG5 with four different continuous deflection set-ups.

III.III. Discussion

III.III.i. Impulsive Deflection of 2007 VK184

The NEO is poised for a close approach to Earth around May 31, 2048 with an impact probability of about 0.055% (from the JPL website data). The asteroid has no planetary flybys between its discovery in 2007 and 2048: the closest approaches are to Venus and Mars in the 2030s, but at distances of several million kilometers. No distortion of the $\Delta\mathbf{v}$ plot (fig. 5) due to such approaches is apparent.

As predicted by the literature, the optimal impulse is very nearly tangential for most of the surveyed date range, rising slowly as the impact approaches and showing a sharp increase in the last orbital period prior to the impact. Fig. 6 shows the deflection values actually obtained: most cases are within the defined tolerance. Two cases, however, failed to converge, although the deviation from the expected value is small. Both failures appear in the last asteroid orbital period, highlighting the difficulties the optimizer experiments in the fast-changing dynamical environment of that final leg of the trajectory.

III.III.ii. Impulsive Deflection of 2011 AG5

The processing of the second NEO is complicated by the fact that the asteroid has a close encounter with Earth itself around February 3, 2023. This flyby greatly augments the uncertainty in the last encounter, so that virtual impactors are found even when the nominal orbit analyzed by NIRAT does not enter the sphere of influence of Earth near that date.

The evolution of the required impulse over time, fig. 7, is similar to the previous case, but with a marked influence of the 2023 flyby. The amplification effect is felt in all prior deflections, with values of the required impulse as low as 0.1 mm/s; up to 1.5 orders of magnitude lower than attempts after the 2023 encounter. As before, the optimal impulse is nearly tangential for most dates, but a few months before the Earth flyby the in-plane normal component dominates.

Additionally, fig. 8 shows that most cases have been successfully processed; but near the end of the range a single case has failed: the achieved deflection is less than 20% of the requested value of 1 $R_E$, invalidating that particular data point.

III.III.iii. Continuous Deflections

Fig. 9 and fig. 10 replicate fig. 2 from Bombardelli and Baù[16], as a test of both NEODET implementation and the accuracy of the analytic approximation proposed in [16]. Note that the resulting magnitudes are not directly comparable with those in the original paper, since the NEODET post-processor normalizes b-plane data with the *scaled planetary radius* $B(v_\infty)$, which is a better measure of the obtained deflection than the raw Earth radius used in [16]. A re-scaling of the axes to match the ones in the mentioned paper would show that the tool results agree with those in the reference.

As described before, the solid lines represent the attempts in which all the time until the impact is used for the actual thrust; while the dashed lines represent cases with a maximum thrust time of two years. The results show the expected behavior: increases in $|\xi|$ depend directly on the thrust being maintained, so the coast phase produces only a small oscillation; while the total deflection grows even when coasting due to the accumulation of the secular drift terms.

## IV. THE RISK MITIGATION STRATEGIES EVALUATION TOOL - RIMISET

The last tool in the risk mitigation suite, RIMISET, is designed to evaluate the performance of different mitigation methods in a particular deflection situation and compare their results based on certain figures of merit. Each mitigation method is supplied with information about the NEO, its trajectory, the available transfers to reach it from Earth and other method-specific information. The program allows two different

problems to be defined, each with a different set of figures of merit:

1. Direct problems, where the methods are allotted a given Earth escape mass for each case, and return the maximum attainable NEO interaction with such a mission. In other words, methods based on impulsive deflections return the largest $\Delta\mathbf{v}$; while those that cause continuous deflections return the longest push time $T_p$ that may be sustained.

2. Inverse problems, where the methods are asked to produce a certain orbital interaction on the NEO given by either of the measures named above, and return the smallest Earth escape mass of the mission that will fulfill the requirements.

The design is thus complementary and in contrast to NEODET, which computed how to deflect a threatening object from the standpoint of *orbital mechanics*. In other words, NEODET quantifies the deflection requirements and RIMISET examines the performances of the methods available to actually create such a deflection. Unlike other tools of the suite, RIMISET has no orbital propagation capabilities, relying on data from other tools and focusing on the implementation of the mitigation methods.

### IV.I. Description

#### IV.I.i. NEO Modeling

In the first two tools, the target object is represented only by its extended state vector (**r**, **v**, *m*). However, most mitigation methods need more detailed information on the NEO. As a minimum, the additional information shared between methods consists of the ephemerides of the unperturbed NEO trajectory (see IV.I.ii) and a model of the object size based on two co-centered spheres of radii $r_a$ and $R_a$, which mark the inner and outer extents of the asteroid surface.

Other information, like data on the properties of the surface material, is method-specific and will be described as required on the relevant subsections.

#### IV.I.ii. Deflection and Orbital Data

All mitigation options in the tool require the output of at least one NEODET case targeting the object in question, as the program is designed to operate over a series of dates which have associated deflection specifications obtained from NEODET. Some methods employ such data even if the program is configured for a direct problem, e.g. the impulse-based methods often use the direction of the optimal impulse in their computations. RIMISET allows the specification of several NEODET results files, which may be assigned to different methods.

Other important information is the specification of the spacecraft state at arbitrary points in time, e.g. to compute the available solar power needed for the operation of some mitigation options (e.g. those using solar electric propulsion). However, given that RIMISET has no orbital propagation facilities, the tool assumes that the S/C orbit follows the same path as the unperturbed NEO. This information is supplied by NEODET in a simplified binary ephemerides format: as the use of this information does not require high levels of precision in this context, the tool merely performs linear interpolation on the ephemerides data.

#### IV.I.iii. Earth–NEO Transfer Handling

The fact that RIMISET must examine how to impart a particular deflection requires the knowledge of the Earth–NEO transfer trajectory; particularly the flight time, the arrival conditions and the amount of fuel consumed by the en-route maneuvers. Given that the tool lacks the features to perform transfer propagations, the task is left to an external Elecnor Deimos tool called SESWIC (Sequential Swing-bys Investigation Code), which produces a large number of transfer solutions to the target NEO including multiple planetary swing-bys and maneuvers. As with deflection files, RIMISET allows the selection of several SESWIC files which are then assigned to different methods using aliases.

#### IV.I.iv. Spacecraft Propulsion Model

Slow-push mitigation methods interact with the threatening object over a long period of time, so the mission spacecraft will need to fly a certain trajectory near the object, which requires a dedicated propulsion subsystem as part of the mission payload. RIMISET models the thrust level from the propulsion subsystem by a constant value $k$ times a time-varying part $f(t)$. Two models are available: a constant-thrust engine and a solar-powered engine, both with constant specific impulse $I_{sp}$. In the former $k$ is the thrust itself and $f \equiv 1$; while in the latter $k$ is the thrust at 1 AU from the Sun and $f$ is the inverse of the square of the distance to the Sun (in AU).

Using the mentioned model, the propellant mass that is spent in a given push time $T_p$ is:

$$\Delta m_p(T_P) = \frac{k_T}{I_{sp} g_0} \int_{t_0}^{t_0+T_P} f(t)\,\mathrm{d}t \qquad [6]$$

Where the sub-index $T$ in the engine reference value stands for the *total* thrust; that is, the combined output of all thrusters using the same model. However, the full engine block includes other elements which are represented in the power plant term $m_{pp}$:

$$m_{pp}(T_P) = \alpha_{pp} F_T \frac{I_{sp} g_0}{2} \frac{1}{\eta_T} \qquad [7]$$

Where $\alpha_{pp}$ is the *inverse power density* of the power plant and $\eta_T$ is the thruster efficiency in converting electric to kinetic power.

Usually, [7] would be defined as the maximum value of that expression in the interval of interest, since both $\alpha_{pp}$ and $F_T$ vary with time. However, in both current models either both are constant, or their form makes the product a constant: in solar engines $F_T \sim r^{-2}$ and $\alpha_{pp} \sim r^2$, with $r$ the distance to the Sun.

Finally, the full propulsion subsystem consists of all the above terms, plus the propellant tanks, represented as a fraction $\kappa_t$ of the spent mass:

$$m_{PL} = m_{pp} + (1+\kappa_t)\Delta m_p \qquad [8]$$

IV.I.v. Deflection by Kinetic Impactor

The principle of a kinetic impactor is simple and well documented in the literature[19]: an object, termed the impactor, crashes at hypervelocity into the NEO causing an impulsive change in its momentum, possibly enhanced by ejected asteroid mass. The impactor properties are straightforward, but the cratering model has been the subject of thorough research[20], with the general consensus stating that both contributions to the momentum are aligned under certain conditions. The model describes the obtained deflection as:

$$\Delta\mathbf{v}_a = \beta\frac{m_{SC}}{m_a}\mathbf{v}_{SC} \qquad [9]$$

Where $\beta$ is the *momentum multiplication factor*, $m_{SC}$ is the S/C mass, $m_a$ is the asteroid mass and $\mathbf{v}_{SC}$ is the relative S/C arrival velocity to the asteroid. $\beta$ models the additional impulse caused by the mass ejection and is computed by RIMISET using a power law model based on research by Housen and Holsapple[21]. The user needs to provide the two model constants $K$ and $\mu$, included in such reference which depend mainly on the NEO surface material and structural properties. In general, porous materials imply smaller values of $\beta$.

For inverse problems, the determination of the computed impulse $\Delta\mathbf{v}_{obt}$ needs to ensure that the NEODET optimal impulse $\Delta\mathbf{v}_{req}$ is achieved. However, since the direction of the impact trajectory is fixed by the transfer, the target impulse is scaled so that its projection in optimal direction fulfils the requirement.

$$\Delta v_{obt}^{inv} = \frac{\Delta\mathbf{v}_{req}}{\cos\alpha}\cdot\frac{\mathbf{v}_{SC}}{v_{SC}} \qquad [10]$$

Where $\alpha$ is the misalignment between the impact trajectory and the optimal direction.

IV.I.vi. Deflection by Nuclear Blast

The obvious next step for impulsive deflections when other methods would not suffice is a nuclear blast. For this method the program employs the model described by Solem[22]. The detonation vaporizes part of the NEO, creating a large crater and causing mass ejection similar to the kinetic impactor.

According to the model, the ejected mass is defined by a power law of the released energy with two constants $A$ and $B$ ($\alpha$ and $\beta$ in the reference), following experimental study of cratering processes. The global ejecta kinetic energy is modeled with another user-provided constant called the energy coupling constant $\Delta$ ($\delta$ in [22]). Thus, RIMISET computes the deflection as:

$$\Delta v_a = \frac{A\Delta}{m_a}\cdot(\varphi m_b)^{\frac{B+1}{2}} \qquad [11]$$

Where $\varphi$ is the yield-to-mass ratio of the bomb. Solem presents this model as valid for any kind of nuclear blast deflection, with different constant values for a surface, buried or stand-off detonation.

The implemented nuclear method accepts both impact transfer trajectories and rendezvous transfers with the NEO: the former case is handled like the kinetic impactor, using [10] in the inverse case to compute the actual deflection target; while in the latter it is assumed that the spacecraft will position itself so that the resulting deflection is fully aligned with the optimal direction.

Note that the variable used by the nuclear deflection method is not the S/C mass at arrival but only the mass of the bomb, that is, the mission payload. Unlike in the kinetic impactor, the structural mass does *not* help towards the deflection target. The transfer handling routines take this distinction into account and add the needed structural mass as required.

IV.I.vii. Deflection with an Ion Beam Shepherd

A slow-push deflection method proposed as recently as 2011, the ion beam shepherd is similar to the gravity tractor but is apparently simpler to execute. The method uses a pair of nearly balanced thrusters to hover at a stable distance from the NEO, either leading or trailing it along its orbit. The object is hit by the exhaust plume of a thruster and is consequently pushed by it.

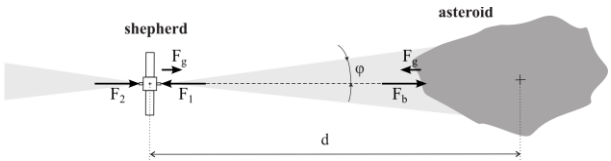

Fig. 11: Diagram of the ion beam shepherd concept.

The model put forward by Bombardelli and Peláez[23] assumes that the spacecraft is far enough from the NEO

for the mutual gravitational interaction to be negligible. This is a strong point of the design because it relaxes the stringent control requirements that are characteristic of gravity tractor designs, as noted in later sections.

The beam force is generated by ionizing interactions at the NEO surface that stop the incoming plume, thus absorbing its momentum with a very high efficiency $\eta_v \sim 1$. Thus, the total thrust employed by the spacecraft is:

$$F_T = \frac{2}{\eta_v} F_a(t) \qquad [12]$$

Where $F_a$ is the same force profile given to generate the NEODET file; the force that the NEO is supposed to receive to produce the desired deflection.

The tool implements the ion beam shepherd by using [12] to find out the total thrust requirements, and then uses the engine model as defined in [6], [7] and [8] to either obtain the required payload mass (for inverse problems) or compute the maximum mission duration given the available payload mass (for direct problems). The use of the transfer routines bridges the gap between the Earth escape mass and the payload mass.

Once the mission has been deemed viable from a payload mass standpoint, the geometric feasibility must be verified. The distance to the NEO must be large enough that the gravitational attraction is negligible; but small enough that the beam is fully intercepted:

$$\sqrt{\frac{\mu_a}{k_g}\left[\frac{m_{SC}}{F_T}\right]_{max}} \le d \le \frac{r_a}{\tan\varphi} \qquad [13]$$

Where $k_g$ is an arbitrary small constant (1% in RIMISET) relating the gravitational and beam forces.

IV.I.viii. Deflection with a Hovering Gravity Tractor

Gravity tractor (GT) deflection missions are based on the idea of using a massive spacecraft as a contact-less tow-ship. This requires the S/C to be in close proximity to the NEO; typical distances in proposed designs are around 2-3·$R_a$. At such a close range, two problems arise:

1. The complexity of the collision avoidance and operational control systems increases, as most NEOs are not spheroidal but markedly triaxial.

2. The exhaust plumes from the thrusters must not impinge on the asteroid surface. A failure to keep this separation would result in transference of momentum to the NEO in the opposite direction, partially (or even completely) counteracting the desired force.

The latter concern has been addressed by two separate GT designs: hoverers and displaced orbiters. The first model, described in this section, was proposed by Lu and Love[24]. It puts the spacecraft either leading or trailing the target in its orbit, with a system of $n$ symmetric thrusters exerting a total force $F_T$. The thrusters, which expel exhaust cones of semi-angle $\varphi$, are all canted away from the NEO orbit tangential direction at an angle $\delta$ (fixed at construction) to clear the NEO surface. The resulting configuration is shown in fig. 12; note that the tangency of the thruster exhaust cones is *not* a requirement.

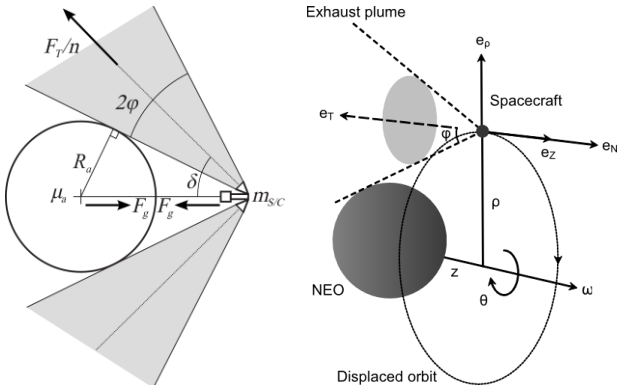


Fig. 12: Hovering (left) and orbiting (right) GTs in the tangent exhaust configuration.

In the model, the instantaneous distance between the spacecraft and the NEO is fixed by:

$$d = \sqrt{\frac{\mu_a}{k_T \cos\delta}\frac{m_{SC}(t)}{f(t)}} \qquad [14]$$

The presence of the canting angle $\delta$ in this formula (and most others) is problematic because it couples the system together. In fact, the applied force profile determines the reference value for the *useful* thrust $k_u = k_T \cos\delta$, instead of $k_T$ itself. This carries over to the mass equations [6] and [7], which require the total thrust and so are left depending on the choice of $\delta$.

As a solution, RIMISET considers that in the worst case (minimum relative distance), the thruster exhaust cone will be *exactly tangent* to the NEO outer surface:

$$d_{\min}^{geom} = \frac{R_a}{\sin(\delta - \varphi)} \qquad [15]$$

With the above, the tool forms an equation for $\delta$ by holding that the minimum distance given by the geometric constraint in [15] must match the actual minimum of the trajectory in [14]. Thus, the main equation is [14] = [15] at a time $t = t^*$ to be determined.

The other constraint in the system is mass-related: the payload mass and the mission running time are linked by [8]. The problem is solved iteratively, with a single variable (which is $T$ for direct or $m_{PL}$ for inverse

problems) used to drive a bisection solver over the geometric equation. The value of $\delta$ used in each iteration comes from applying the requested force profile and the current value of the bisection variable to the payload mass definition.

Finally, analysis of [14] shows that the minimum distance occurs at the time $t^*$ with the minimum $m_{SC}/f$ ratio. It is straightforward for missions with a constant-thrust engine: the S/C mass decreases linearly and $f = 1$, so the minimum separation occurs at $t^* = t_f$. However, the use of a solar-powered engine complicates the problem of finding $t^*$ significantly. Differentiation of $d$ in that case produces an equation for $t^*$ that depends on the distance and radial velocity to the Sun. The tool sweeps the interval of interest, looking for the global minimum of the mutual distance by detecting changes of sign in that equation and computing the distance to compare between two local minima.

IV.I.ix. Deflection with an Orbiting Gravity Tractor

The second GT design[25] avoids the canting of the S/C thrusters, instead establishing a displaced circular orbit of radius $\rho$ and displacement $z$ around the NEO so the secular gravitational force is in the same direction as before. The design choice in this case consists of keeping the exhaust cone tangent to the NEO outer radius at all times, which produces:

$$R_a = \rho\cos\varphi - z\sin\varphi$$
$$F_T = \mu_a m_{SC}\frac{z}{\left(\rho^2+z^2\right)^{2/3}} \qquad [16]$$

The geometric and mass equations are uncoupled, since the force profile to apply is known a priori. This allows a solution algorithm similar to that of the ion beam shepherd, where the mass data is computed first and then the geometric compatibility is verified. The tool performs this test by isolating $\rho$ from the expressions in [16] and then equating both values.

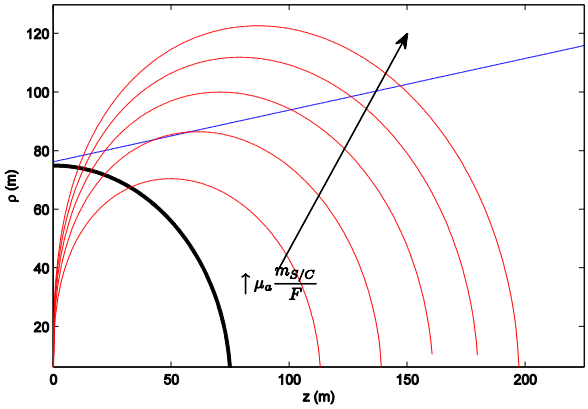


Fig. 13: Geometric constraints in the orbiting GT.

Analysis of the constraints reveals that the existence of a solution for a given point in time is determined by the value of the gravitational parameter $\mu_a \cdot m_{SC}/F$. As displayed on fig. 13, this dependency is monotonic: the larger the gravitational parameter, the larger the maximum $\rho_{grav}$, so the worst case will occur when this parameter is smallest. This reduces to finding the minimum $m_{SC}/F$, so RIMISET uses the same code as in the hovering GT to find the worst instant $t^*$ and test the feasibility of the case.

IV.II. Results

Fig. 14 and fig. 15 show the results of two full analyses performed by RIMISET on the feasibility of deflecting 2007 VK184 and 2011 AG5, respectively. The attempts start in early 2014 and are tried once every 16 days until the impact date.

Deflection data for impulsive methods was reused from III.II.i, while information for the slow-push methods was regenerated with a still high but more realistic thrust profile. The employed thruster is based on NASA's Evolutionary Xenon Thruster[26], with slightly modified values of $I_{sp}$ = 4200 s, a constant tangential thrust of 0.25 N and $\eta_T$ = 50%, with an exhaust divergence semi-angle of around 10º. The power system is assumed to require 0.02 kg/W and the tanks weigh 7% of the propellant mass.

Only NEODET outputs which achieve the desired deflection are sampled, causing the slow-push methods to vanish from the plot years before the impact. All methods employ values near those suggested in their respective literatures for any required model constants, see [21], [22] and [23]. Finally, the nuclear bomb is assumed to yield 1 $kton_{TNT}$ per kilogram of the full assembly.

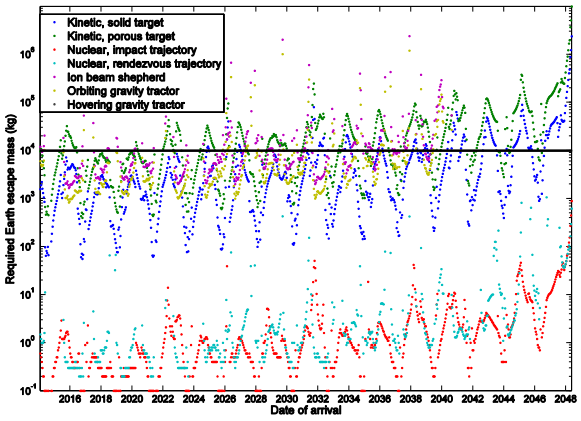


Fig. 14: Earth escape mass required by different prospective missions to deflect 2007 $VK_{184}$ for a range of dates of arrival to the NEO.

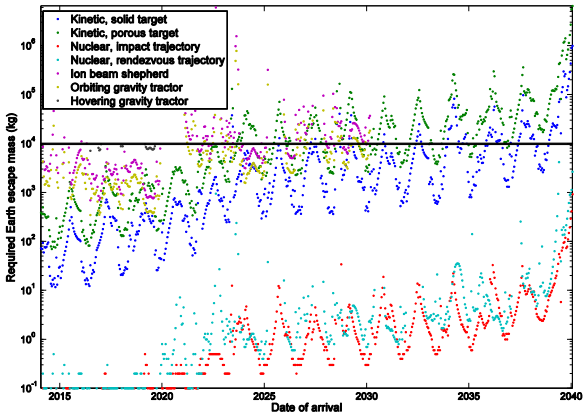


Fig. 15: Earth escape mass required by different prospective missions to deflect 2011 $AG_5$ for a range of dates of arrival to the NEO.

IV.III. Discussion

A glance at fig. 14 and fig. 15 shows that, if the Earth escape mass of the probe were the only figure of merit in the choice of the mission to send, the nuclear option would be the clear winner – even considering that the model constants chosen by Solem may be too optimistic. However, external considerations like the dubious safety of strapping a nuclear weapon onto a launcher that may fail to reach an escape trajectory, suggest leaving the nuclear option as the last resort.

Of the other methods, kinetic deflections arise as the most versatile because they are feasible for both asteroids with reasonable transfers and masses until the very last period of the NEO. Furthermore, kinetic impactors profit significantly from the perturbation amplification effect of a possible flyby after the deflection, as shown in fig. 15 in the years 2014−2023. On the other hand, the achieved deflection is strongly dependent on the computed value of $\beta$, which is subject to a large level of uncertainty (blue vs. green series in the graphs), so the method is not useful if a precise deflection is required.

Finally, slow-push methods allow a finer control and monitoring of the NEO deflection, but in most cases they require large Earth escape masses that do *not* receive the advantages of a previous flyby as clearly as impulsive methods. This is due to the fact that only the spent propellant mass [6] shrinks in pre-flyby deflection attempts (because the push time is much shorter), but the power plant mass [7] is driven by thruster parameters which do not necessarily change.

## V. CONCLUSIONS

This paper presents the suite of tools developed by Elecnor Deimos in the frame of the NEOShield FP7 project for the analysis of mitigation solutions and mission design options required to alleviate the risk posed by threatening NEOs. This suite is composed by three tools that respectively allow determining if an asteroid is to collide with Earth (NIRAT tool), compute the required object deflection (NEODET tool) and assess the design features of the possible mitigation space missions (RIMISET tool).

Design solutions, methods and algorithms employed and the overall set-up of the tools have been presented. Results from all the tools have been obtained by a chained execution of the different tools in application to two well known asteroids: 2011 AG5 and 2007 VK184. The obtained results allow comparing the design and performance requirements associated to different deflection methods and thus favor the selection of the best option for a space mitigation mission.

[1] NEODys web page, http://newton.dm.unipi.it/neodys/ , last data collection date Sep. 12th, 2012

[2] JPL NEO Program web page, http://neo.jpl.nasa.gov/ , last data collection date Sep. 12th, 2012

[3] P.W. Chodas and D.K.Yeomans, Predicting Close Approaches and Estimating Impact Probability for Near Earth Objects, AAS/AIAA Astrodynamics Specialists Conference, Girdwood, Alaska, 16-19 Aug. 1999

[4] A. Milani, S.R. Chesley, P.W. Chodas, and G.B. Valsecchi Asteroid Close Approaches: Analysis and Potential Impact Detection, Chapter in Asteroids III, 2002

[5] A. Milani, S.R. Chesley, M.E. Sansaturio, G.Tommei, G.B. Valsecchi, Nonlinear Impact Monitoring: Line of Variation Searches for Impactors, Icarus, 173 (2), 2005

[6] NEODYS-2 Impact risk page, http://newton.dm.unipi.it/neodys/index.php?pc=4.1, last data collection date September 12th, 2012

[7] Sentry Impact Risk Page, http://neo.jpl.nasa.gov/risk/, last data collection date September 12th, 2012

[8] E. Fehlberg, Classical Fifth-, Sixth-, Seventh- and Eight-Order Runge-Kutta Formulas with Stepsize Control (Technical Report R-287), NASA, 1968

[9] T.D. Moyer, Mathematical Formulation of the Double-Precision-Orbit-Determination-Program (DPODP), Issue 32, Part 1527 of JPL technical report, 1971

[10] M. Matsumoto, T. Nishimura, Mersenne twister: a 623-dimensionally equidistributed uniform pseudo-random number generator, ACM Transactions on Modeling and Computer Simulation 8 (1) (1998), 3–30

[11] G.E.P. Box and Mervin E. Muller, A Note on the Generation of Random Normal Deviates, The Annals of Mathematical Statistics (1958), Vol. 29, No. 2 pp. 610–611

[12] A. Milani, M.E. Sansaturio, G. Tommei, O. Arratia, and S.R. Chesley, Multiple Solution for asteroid Orbits: Computational Procedure and Applications, A&A 431 (2005), 729–746

[13] D. Morrison, C.R. Chapman, D. Stee, and R.P. Binzel, Impacts and the Public: Communicating the Nature of the Impact Hazard, in Mitigation of Hazardous Comets and Asteroids, Cambridge University Press, 2004

[14] J.D. Giorgini, L.A.M. Benner, S.J. Ostro, M.C. Nolan, M.W. Busch, Predicting the Earth Encounters of (99942) Apophis, Icarus 193 (2008), 1-19

[15] S.R. Chesley, Potential Impact Detections for Near-Earth Asteroids: the Case of 99942 Apophis (2004MN4), Asteroids, Comets, Meteors, Proceedings IAU Symposium No. 229, 2005

[16] C. Bombardelli and G. Baù, Accurate analytical approximation of asteroid deflection with constant tangential thrust, Celestial Mechanics and Dynamical Astronomy, 114, 3, pp. 279-295, 2012

[17] S. Adlaj, An Eloquent Formula for the Perimeter of an Ellipse, Vol.59 N.8 Not. Am. Math. Soc., 2012

[18] G. Bellei, J.L. Cano, Kinetic Impact Mitigation Options for Asteroid 2011 AG5, Elecnor Deimos, February 2012, http://www.space-explorers.org/committees/NEO/2012/AG5_Deimos_analysis_13Feb12.pdf

[19] K. Holsapple, The scaling of impact processes in planetary sciences, Ann. Rev. Earth Planet. Sci, 1993

[20] K. Holsapple, I. Giblin, K. Housen, A. Nakamura and E. Ryan, Asteroid impacts: laboratory experiments and scaling laws, 2002

[21] K. Holsapple and K. Housen, Deflecting asteroids by impacts: what is ß?, 43rd Lunar and Planetary Science Conference, 2012

[22] J.C. Solem, Interception of comets and asteroids on collision course with Earth, Journal of Spacecraft and Rockets vol. 30, 1993

[23] C. Bombardelli and J. Peláez, Ion Beam Shepherd for Asteroid Deflection, Journal of Guidance, Control and Dynamics vol. 34, 2011. arXiv:1102.1276

[24] E. Lu and S. Love, Gravitational tractor for towing asteroids, Nature, Vol. 438 No. 7065 pp. 177–178, 2005

[25] C.R. McInnes, Near Earth object orbit modification using gravitational coupling, Journal of Guidance, Control and Dynamics vol. 30, 2007

[26] D.A. Herman, NASA's Evolutionary Xenon Thruster (NEXT) Project Qualification Propellant Throughput Milestone: Performance, Erosion, and Thruster Service Life Prediction After 450 kg, Glenn Research Center. NASA/TM—2010-216816.